Solid State Communications 149 (2009) 670 672

Contents lists available at ScienceDirect

Solid State Communications

journal homepage: www.elsevier.com/locate/ssc

Microscopic origin of current degradation of fully-sealed carbon-nanotube field emission display

Seungchul Kim [a], Eunae Cho [b], Seungwu Han [b], Youngmi Cho [c], Sung Hee Cho [c], Changwook Kim [c], Jisoon Ihm [a,*]

[a] Department of Physics and Astronomy, FPRD, Seoul National University, Seoul 151-747, Republic of Korea
[b] Department of Physics, Ewha Womans University, Seoul 120-750, Republic of Korea
[c] CAE Team, R&D Center, Samsung SDI, Yongin 446-577, Republic of Korea

ARTICLE INFO

Article history:
Received 21 January 2009
Accepted 21 February 2009
by J.R. Chelikowsky
Available online 3 March 2009

PACS:
79.70.+q
61.46.-w
31.15.A-

Keywords:
A. CH_3 radical
D. Current degradation
D. Field emission display

ABSTRACT

The current-degradation mechanism of a fully sealed, carbon-nanotube field emission display is investigated experimentally and theoretically. From residual gas analysis, it is strongly evidenced that CH_3 radicals from the organic materials in the paste deteriorate emission properties. Based on *ab initio* methods, it is found that CH_3 radicals can increase electrical resistance of the nanotube and suppress emission currents. In addition, molecular dynamics simulations demonstrate that thermal destruction of CH_3-attached nanotubes occurs at lower temperatures than for pristine nanotubes. Our results suggest that the material selection of the paste is crucial for extending the lifetime of nanotube-based field emission displays.

1. Introduction

Owing to their unique advantages as electron emitters, carbon nanotubes (CNTs) are considered as ideal materials to be used for emission tips in the field emission display (FED). For example, CNTs possess a high aspect ratio ranging up to several thousands, which facilitates the field emission. In addition, the ballistic conduction of the CNT ensures that the temperature of the emission tip does not rise too high during the field emission, which is essential for an extended lifetime and performance stability. After the original fully-sealed prototype of the CNT-FED was announced in 1999 [1], significant technological advances have been achieved to improve the image quality at higher resolutions. Most recently, a 15-in. full color display was demonstrated [2].

In spite of the impressive progress in such a short period, there are still several technical issues such as cell-to-cell uniformity or display lifetime which should be resolved for the CNT-FED to compete with other commercial displays. In particular, the lifetime issue would constitute a very serious obstacle [3 5]. Interestingly, this is in contrast with a general perception that the CNT is a strong material that can endure the extreme conditions of the field emission. When the degradation of the CNT was studied with scanning probes, the failure mechanism was found to be intrinsic factors such as resistive heating, mechanical stress or field evaporation [6 8]. On the other hand, in a fully sealed device, extrinsic origins such as residues from binders or phosphors seem to significantly degrade the emission currents [4,5,9]. However, as yet the microscopic understanding is not satisfactory. In this work, based on a series of experimental and theoretical analysis, it is proposed that radicals such as CH_3 are more responsible for the current degradation in the fully-sealed CNT-FED than any other sources.

2. Experimental results

We fabricate a 5-in. CNT-FED using screen-printing and firing methods [2,10,11]. The emitter is formed using the CNT paste made from CNT powders and functional additives. We used bundles of single-walled CNT produced by HiPCO method (Carbon Nanotechnologies, Inc.). The CNT-FED is based on the triode-type top-gate structure that includes an additional gate to improve electron focusing. The current versus operation time is measured as shown in Fig. 1. It is found that the current level decays significantly over hundreds of hours, which is much shorter than the lifetime required for commercial displays.

* Corresponding author. Tel.: +82 2 880 6614; fax: +82 2 884 3002.
E-mail address: jihm@snu.ac.kr (J. Ihm).

0038-1098/$ see front matter © 2009 Elsevier Ltd. All rights reserved.
doi:10.1016/j.ssc.2009.02.025

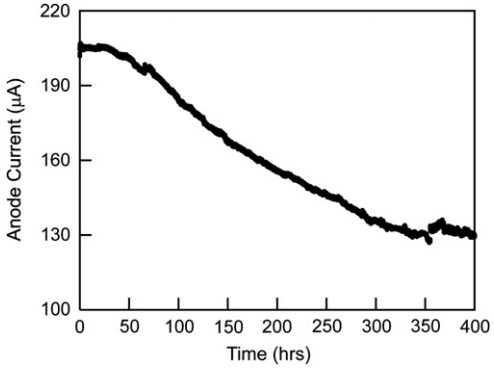

Fig. 1. Emission currents with respect to the running time of the 5-in. triode-type FED with an applied voltage of 5 kV.

Table 1
Residual gas analysis of fully-sealed, carbon-nanotube field emission display.

Residual gases	H_2	CO	N_2	CH_4	H_2O	C_2H_6	Ar	CO_2
Partial pressure ($\times 10^{-7}$ Torr)	13.4			286	0.227	1.5	16.6	2.51
Mass ratio (%)	4.2			89.29	0.07	0.47	5.19	0.78

In order to investigate the degradation mechanism, the composition of residual gases was analyzed after 50 h of field emission. The measurement was performed with a RGA analysis system by Piper Vacuum and the results are shown in Table 1. It is striking that residual gases are dominated by methane (CH_4) molecules, covering 90% of the total mass; before the device operation, the field emission display was fully sealed with the vacuum level of 10^{-7} Torr and CH_4 gas was negligible in the initial residual gas analysis. In comparison, CO and CO_2 accounts for an extremely small portion of the residual gas. This indicates that oxygen atoms or molecules may not be deeply involved in the current degradation of a fully-sealed CNT-FED. The detection of CH_4 molecules strongly implies the generation of radicals, most probably the methyl radical (CH_3). During the out-gassing process, CH_3 may combine with other hydrogen species to result in a more stable form of CH_4.

The source of the CH_3 radical is believed to be the organic paste. Besides CNTs, the paste materials are composed of binder polymers (acrylate or cellulose), sensitizers and solvents, which contain aliphatic chains (repetition of CH_2). The TGA analysis on the paste material showed that these polymers start to dissociate at 620 K and are fully disintegrated around 720 K. The temperature of the paste during the device operation is not available at present. However, there are several experiments supporting the high temperatures of CNTs during field emission. For example, it was reported in Ref. [12] that the temperature of CNTs can increase up to 1550 K when the current density is 1 mA/cm^2, a typical value required for FED. Considering that the CVD method used in this reference form a better CNT-electrode contact than for the paste method, the local temperature of the paste in contact with CNTs could increase above the dissociation point (∼700 K). The dissociation process involves the breakdown of aliphatic chains in the polymers, which should generate CH_x ($x =$ 1 3) radicals. Although various radical species can be produced by the degradation of organic polymers, the CH_3 radical might be a dominant one, resulting in stable CH_4 (CH_3+H) or C_2H_6(CH_3+CH_3) molecules as shown in Table 1.

3. Theoretical analysis

Because the CH_3 radical is an extremely active molecule, it is likely that a substantial amount of the gas interacts with the CNT

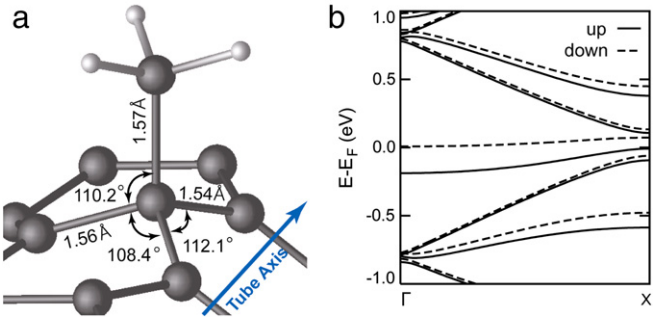

Fig. 2. (a) Adsorption geometry of CH_3 on the side wall of the (5,5) nanotube. (b) The spin-decomposed band structure of the (5,5) CNT with one CH_3 attached to every eight unit cells.

near the cap region or at the side wall. Since it is difficult to isolate the effect of radicals in experiment, *ab initio* calculations and molecular dynamics (MD) simulations are employed to investigate the emission properties and stabilities of CH_3-attached CNTs. For *ab initio* calculations, the SIESTA code is used [13]. The spin-polarized generalized gradient approximation is adopted to describe the exchange-correlation energy of electrons [14]. Double-ζ basis sets are used with an energy cutoff of 160 Ry for constructing a real-space mesh. All atoms are fully relaxed until the atomic force on each atom is reduced to 0.04 eV/Å. For classical MD simulations, the Tersoff Brenner potential is used since it is known to describe hydrocarbon systems reliably [15].

First, it is studied how CH_3 affects electronic properties of the CNT. To this end, a methyl radical is attached to every eight unit cells of the (5,5) CNT, corresponding to a coverage of 0.6%. Various configurations are tested and the radical is found to be most stable on top of a carbon atom [see Fig. 2(a)]. The computed adsorption energy is 1.19 eV, which compares with 2.57 eV obtained with the local density approximation [16]. The overall bonding angles and lengths around CH_3 indicate a sp^3-bonding character. The band structure of the CH_3-attached CNT in Fig. 2(b) shows that quasi-bound states are formed at the Fermi level, effectively opening an energy gap between π- and π^*-bands. The band splitting of quasi-bound states can be explained by the Stoner criteria in the same manner as a hydrogen atom adsorbed on the graphene sheet [17]. The localized states right at the Fermi level increase the resistance because any defect state in a ballistic conductor reduces the conductance. Furthermore, the resistance of the CNT reduces the field enhancement factor at the tip end, suppressing the emission currents substantially.

Next, it is examined how emission properties are affected when CH_3 radicals are bound at the nanotube tip. The magnitude of emission currents depends strongly on the atomic and electronic structures in the tip region. In particular, it has been proposed that localized states at the end of the CNT contribute to emission currents substantially [18,19]. To study how distributions of localized states are affected by the radicals, the electronic structures are calculated on the nanotube tips with CH_3 radicals attached in various concentrations. The (5,5) CNT with the hemisphere of C_{60} capping at one end of the nanotube (see Fig. 3) is considered. The length of the CNT is ∼36 Å and the other side of the CNT is passivated with hydrogen atoms. When a CH_3 radical is adsorbed at the cap region of the CNT, the binding energies are 1.26 1.85 eV, which are larger than for the side-wall adsorption. If five radicals are attached simultaneously, the adsorption energy per CH_3 unit slightly increases to 2.09 eV. This suggests that a large number of CH_3 could be bound at the emission tip.

The projected density of states (PDOS) on atoms in the C_{60} hemisphere and radicals are shown in Fig. 3(b) for a representative configuration of CH_3 adsorption. In the absence of the external

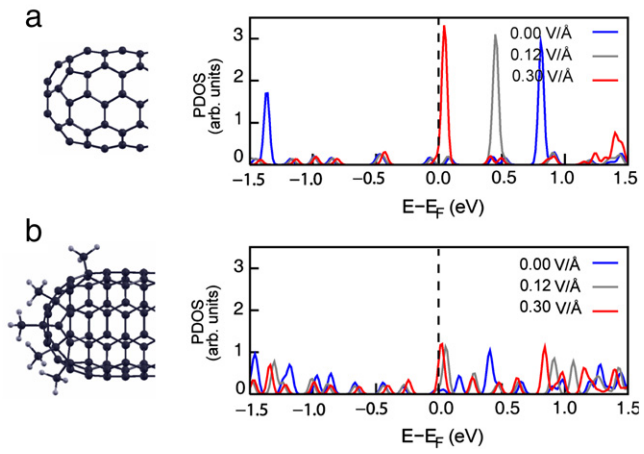

Fig. 3. (Color online) The atomic configuration of (a) clean and (b) CH_3-bound (5,5) nanotube tips and corresponding partial density of states (PDOS) projected onto the hemisphere of C_{60} and CH_3.

field, the PDOS of a clean nanotube in Fig. 3(a) shows a localized state above the Fermi level. At field emission conditions with an external field of 0.12 or 0.3 V/Å, the localized states shift down and contribute to the emission currents [19]. In the CH_3-attached nanotube under the same external fields, the population of localized states at the Fermi level is substantially smaller than for the clean nanotube. Similar results are found for other concentrations of radicals. This again strongly implies that the emission current of the CNT should be reduced when the nanotube is exposed to CH_3 radicals.

Finally, the structural stability of the CH_3-attached CNT is investigated by carrying out MD simulations. The total simulation time is 10 ps and the temperature is controlled by the Langevin thermostat. To observe thermal destruction processes within the simulation time, the temperature is increased up to 5000 K, much higher than the actual temperature in the device, which is around 1500 K as discussed above. Therefore, the MD results only demonstrate the relative stability among different structures. Fig. 4(a) and (b) show snapshots at the end of MD simulations for the clean and CH_3-attached CNTs, respectively. It is seen that the clean CNT is robust up to 5000 K. In contrast, the CH_3-attached CNT breaks up at lower temperatures around 4000 K. In particular, the ``melting'' of the CNT starts at the tip end, which is a result of weaker bonds in this region. Even though the attached radicals desorb mostly in the form of CH_3, the weakened carbon carbon bonding results in the creation of several dangling bonds and topological defects such as heptagons or octagons. The large chemical activity of these defects will introduce a disordered sp^3 bonding network, especially in nanotube bundles, which can be regarded as an initial step toward the amorphization. This is consistent with a recent experimental observation that the current degradation of the CNT-FED was concurrent with the material transformation from crystalline nanotubes to amorphous carbon materials [5].

4. Conclusion

In summary, it was proposed that CH_3 radicals that originate from organic materials are responsible for the current degradation in a fully-sealed CNT-FED. Experimentally, this was evidenced by residual gas analysis. Various theoretical results also supported that CH_3 degrades the current density and structural stability of the nanotube tip. Considering that the screen printing method is an industrially important process to achieve large-scale production, the control of paste materials will be crucial for increasing the device lifetime. For example, adding a radical scavenger in the paste could prevent the current degradation.

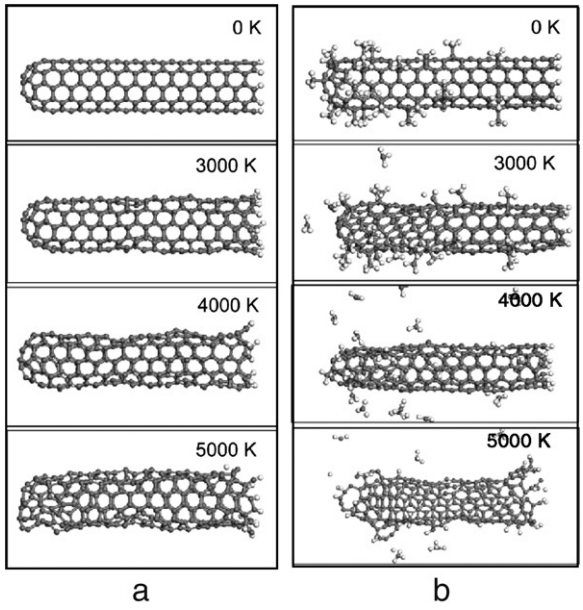

Fig. 4. Snapshots of (a) pristine and (b) CH_3-attached carbon nanotubes after 10 ps of molecular dynamics simulations at various temperatures.

Acknowledgments

This work was supported by Samsung SDI SNU Display Innovation Program (SSDIP). S.K. and J.I. are supported by the SRC Program (Center for Nanotubes and Nanostructured Composites) of MOST/KOSEF. The CNT-FED was produced and tested by the Display Lab of Samsung SDI. Computations were performed through the support of KISTI.

References

[1] W.B. Choi, D.S. Chung, J.H. Kang, H.Y. Kim, Y.W. Jin, I.T. Han, Y.H. Lee, J.E. Jung, N.S. Lee, G.S. Park, J.M. Kim, Appl. Phys. Lett. 75 (1999) 3129.
[2] E.J. Chi, C.H. Chang, J.H. Park, C.G. Lee, C.H. Lee, D.J. Yoo, Y.C. You, D.S. Zang, D.H. Choe, SID Symp. Dig. (2006) 63-1.
[3] J.-M. Bonard, J.-P. Salvetat, T. Stöckli, L. Forró, A. Châtelain, Appl. Phys. A 69 (1999) 245.
[4] S. Lee, D.Y. Jeon, Appl. Phys. Lett. 88 (2006) 063502.
[5] J.H. Lee, S.H. Lee, W.S. Kim, H.J. Lee, J.N. Heo, T.W. Jeong, C.W. Baik, S.H. Park, S. Yu, J.B. Park, Y.W. Jin, J.M. Kim, H.J. Lee, J.W. Moon, M.A. Yoo, J.W. Nam, S.H. Cho, J.S. Ha, T.I. Yoon, Appl. Phys. Lett. 89 (2006) 253115.
[6] J.-M. Bonard, C. Klinke, K.A. Dean, B.F. Coll, Phys. Rev. B 67 (2003) 115406.
[7] Z.L. Wang, R.P. Gao, W.A. de Heer, P. Poncharal, Appl. Phys. Lett. 80 (2002) 856.
[8] L. Nilsson, O. Groening, P. Groening, L. Schlapbach, Appl. Phys. Lett. 79 (2001) 1036.
[9] D.-H. Kim, H.-S. Yang, H.-D. Kang, H.-R. Lee, Chem. Phys. Lett. 368 (2003) 439.
[10] W.B. Choi, Y.W. Jin, H.Y. Kim, S.J. Lee, M.J. Yun, J.H. Kang, Y.S. Choi, N.S. Park, N.S. Lee, J.M. Kim, Appl. Phys. Lett. 78 (2001) 1547.
[11] W.S. Kim, J. Lee, T.W. Jeong, J.N. Heo, B.Y. Kong, Y.W. Jin, J.M. Kim, Appl. Phys. Lett. 87 (2005) 163112.
[12] M. Sveningsson, M. Jönsson, O.A. Nerushev, F. Rohmund, E.E.B. Campbell, Appl. Phys. Lett. 81 (2002) 1095.
[13] J.M. Soler, E. Artacho, J.D. Gale, A. García, A. Junquera, P. Ordejón, D. Sánchez-Portal, J. Phys. Condens. Matter 14 (2002) 2745.
[14] J.P. Perdew, K. Burke, M. Ernzerhof, Phys. Rev. Lett. 77 (1996) 3865.
[15] D.W. Brenner, Phys. Rev. B 42 (1990) 9458.
[16] F. Li, Y. Xia, M. Zhao, X. Liu, B. Huang, Z. Tan, Y. Ji, Phys. Rev. B 69 (2004) 165415.
[17] O.V. Yazyev, L. Helm, Phys. Rev. B 75 (2007) 125408.
[18] S. Han, J. Ihm, Phys. Rev. B 61 (2000) 9986.
[19] S. Han, J. Ihm, Phys. Rev. B 66 (2002) 241402.